EE6104 CA1 Report: Adaptive Control with Only Input & Output Measurable

Hongxuan Wang
A0228929M
hongxuanwang@u.nus.edu

Abstract

An adaptive controller for a continuous-time system with only input and output measurable is designed. Simulations are conducted using MATLAB Simulink. Different filtering parameters are tested, and different reference signals (e.g., square waves and sinusoidal waves with different amplitudes and frequencies) are tested. In addition, a plant change simulation is also conducted to verify the effectiveness of the designed controller. Intermediate data and MATLAB/Simulink files are available at: `https://github.com/hxwangnus/EE6104-Adaptive-Control.git`.

1 Preliminaries

In CA1 project, it is desired to design an adaptive controller for a continuous-time second-order system with only input and output measurable.

The transfer function of the plant is given as:

$$\frac{Y(s)}{U(s)} = \frac{b_0 s + b_1}{s^2 + a_1 s + a_2}, \tag{1}$$

where a_1, a_2, b_0, b_1 are unknown parameters and $b_0 < 0$, and the plant has no zeros in the right-half of the s-plane.

The plant model in the time domain can be derived as:

$$(p^2 + a_1 p + a_2) y(t) = (b_0 p + b_1) u(t), \tag{2}$$

let,

$$R_p(p) = p^2 + a_1 p + a_2, \tag{3}$$

$$Z_p(p) = p + \frac{b_1}{b_0}, \tag{4}$$

$$k_p = b_0, \tag{5}$$

the time domain equation becomes:

$$R_p(p) y(t) = k_p Z_p(p) u(t). \tag{6}$$

To design the adaptive controller with only input and output measurable, a model reference system should be built. The transfer function for the reference model is designed as:

$$H_m(s) = \frac{1}{\tau s + 1} = \frac{1/\tau}{s + 1/\tau}, \tag{7}$$

which is strictly positive real.

The reference model in the time domain can be derived as:

$$(p + \frac{1}{\tau})y_m(t) = \frac{1}{\tau}r(t), \tag{8}$$

where $r(t)$ is the reference signal. Let,

$$R_m(p) = p + \frac{1}{\tau}, \tag{9}$$

$$k_m(p) = \frac{1}{\tau}, \tag{10}$$

the time domain equation becomes:

$$R_m(p)y_m(t) = k_m(p)r(t). \tag{11}$$

The rest of the report is arranged as follows. Section 2 solved task (a), where the adaptive law is designed. Section 3 solved task (b) and task (c), where the simulations are performed using Simulink.

2 Algorithm for the designed adaptive controller

2.1 Non-adaptive control law

To design an adaptive control algorithm, the non-adaptive control law is used as a reference, which is derived in this section.

$R_p(p)$ and $R_m(p)$ can be connected using a division relationship:

$$T(p)R_m(p) = R_p(p)E(p) + F(p), \tag{12}$$

given $R_m(p)$ and $R_p(p)$ known, unique $E(p)$ and $F(p)$ can be determined.

Multiply $E(p)$ on both sides of Eq. (6) gives:

$$E(p)R_p(p)y(t) = k_pE(p)Z_p(p)u(t), \tag{13}$$

combining Eq. (12) and Eq. (13) gives:

$$(T(p)R_m(p) - F(p))y(t) = k_pE(p)Z_p(p)u(t), \tag{14}$$

then

$$R_m(p)y(t) = k_p(\frac{E(p)Z_p(p)}{T(p)}u(t) + \frac{F(p)}{k_pT(p)}y(t)). \tag{15}$$

Define:

$$\bar{G}(p) = E(p)Z_p(p), \tag{16}$$

$$G_1(p) = \bar{G}(p) - T(p), \tag{17}$$

$$\bar{F}(p) = \frac{F(p)}{k_p}, \tag{18}$$

then Eq. (15) becomes:

$$R_m(p)y(t) = k_p(\frac{G_1(p)}{T(p)}u(t) + \frac{\bar{F}(p)}{T(p)}y(t) + u(t)) = k_pk^*r(t). \tag{19}$$

The non-adaptive control law is then:

$$u(t) = -\frac{G_1(p)}{T(p)}u(t) - \frac{\bar{F}(p)}{T(p)}y(t) + k^*r(t). \tag{20}$$

Considering a second-order system, then:

$$G_1(p) = g_1p + g_2, \tag{21}$$

$$\bar{F}(p) = f_1p + f_2. \tag{22}$$

Let $1/T(s)$ be the transfer function of a filter system, the filtered result for control input $u(t)$ is:

$$\omega_u(t) = \frac{1}{T(p)}u(t), \tag{23}$$

and the filtered result for system output $y(t)$ is:

$$\omega_y(t) = \frac{1}{T(p)}y(t). \tag{24}$$

given:

$$T(p) = p^2 + t_1 p + t_2, \tag{25}$$

$$t_1 = 2C\omega, \quad t_2 = \omega^2, \tag{26}$$

where C is the damping ratio and ω is the natural frequency of the system.

Then Eq. (20) becomes:

$$u(t) = -(g_1 p + g_2)\omega_u(t) - (f_1 p + f_2)\omega_y(t) + k^* r(t). \tag{27}$$

Let,

$$\bar{\theta}^* = [-f_2, -f_1, -g_2, -g_1, k^*]^T, \tag{28}$$

$$\bar{\omega} = [\omega_y, p\omega_y, \omega_u, p\omega_u, r]^T, \tag{29}$$

Eq. (27) becomes:

$$u(t) = \bar{\theta^*}^T \bar{\omega}(t) \tag{30}$$

2.2 Adaptive law with only input and output measurable

As in a system with only input and output measurable, k^* is unknown, the optimal control gain $\bar{\theta}^*$ should be replaced by the time-varying control gain $\bar{\theta}(t)$, where:

$$\dot{\bar{\theta}}(t) = -sgn(k^*)\Gamma\bar{\omega}(t)e_1(t). \tag{31}$$

The proof of convergence is derived as follows. Let:

$$\bar{\Phi}(t) = \bar{\theta}(t) - \bar{\theta^*} \tag{32}$$

be the gain error, and

$$e_1(t) = y(t) - y_m(t) \tag{33}$$

be the tracking error, then:

$$R_m(p)e_1(t) = k_p\bar{\Phi}^T(t)\bar{\omega}(t). \tag{34}$$

Define:

$$\omega = [\omega_y, p\omega_y, \omega_u, p\omega_u]^T, \tag{35}$$

which is the non-minimal realization of the plant. Filter the plant using $1/T(s)$ gives:

$$R_p(p)\omega_y = k_p Z_p(p)\omega_u, \tag{36}$$

$$p^2\omega_y = -a_1 p\omega_y - a_2\omega_y + b_0 p\omega_u + b_1\omega_u. \tag{37}$$

Also, by definition,

$$y = T(p)\omega_y = (T(p) - R_p(p))\omega_y + k_p Z_p(p)\omega_u. \tag{38}$$

Combining Eq. (23), (37), and (38), the state-space representation of the plant is:

$$\dot{\omega} = A_p\omega + B_p u, \quad y = C_p^T\omega, \tag{39}$$

where:

$$A_p = \begin{pmatrix} 0 & 1 & 0 & 0 \\ -a_2 & -a_1 & b_1 & b_0 \\ 0 & 0 & 0 & 1 \\ 0 & 0 & -t_2 & -t_1 \end{pmatrix}, \tag{40}$$

$$B_p = \begin{pmatrix} 0 \\ 0 \\ 0 \\ 1 \end{pmatrix}, \tag{41}$$

$$C_p = \begin{pmatrix} t_2 - a_2 \\ t_1 - a_1 \\ b_1 \\ b_0 \end{pmatrix}. \tag{42}$$

The non-minimal realization of the reference model can be derived using the same filter $1/T(s)$:

$$\dot{\omega_m} = A_m \omega_m + B_m r, \quad y_m = C_m^T \omega_m. \tag{43}$$

Let:

$$e = \omega - \omega_m, \tag{44}$$

then

$$e_1 = y - y_m = C_m^T e. \tag{45}$$

Define a Lyapunov equation as:

$$V = \frac{1}{2}(e^T P e + \bar{\Phi}^T \Gamma^{-1} \bar{\Phi}), \tag{46}$$

where

$$A_m^T P + P A_m = -Q, \tag{47}$$

where Q is any symmetric positive definite matrix, and Γ is a positive definite diagonal matrix.

Convergence proof requires $\dot{V} < 0$ for non-zero e, where

$$\dot{V} = -\frac{1}{2} e^T Q e + e^T P \frac{1}{k^*} B_m \bar{\Phi}^T \bar{\omega} + \bar{\Phi}^T \Gamma^{-1} \dot{\bar{\Phi}}. \tag{48}$$

Given the reference model is strictly positive real,

$$P \frac{1}{|k^*|} B_m = C_m, \tag{49}$$

Eq. (48) becomes

$$\dot{V} = \frac{1}{2} e^T Q e + sgn(k^*) e_1 \bar{\Phi}^T \bar{\omega} + \bar{\Phi}^T \Gamma^{-1} \dot{\bar{\Phi}}. \tag{50}$$

As $\dot{\bar{\Phi}} = \dot{\bar{\theta}} - \dot{\bar{\theta}}^* = \dot{\bar{\theta}}$, using adaptive law (Eq. (31)), then Eq. (50) becomes:

$$\dot{V} = -\frac{1}{2} e^T Q e \leq 0, \tag{51}$$

which means V is bounded for all t, and e, $\bar{\Phi}$ are bounded.

According to Eq. (44), as e is bounded, ω is also bounded, then u is also bounded. According to Eq. (45), as e is bounded, e_1 is also bounded, then y is also bounded. This proves the boundedness of the input and output of the system.

In addition, let:

$$\alpha(e, \bar{\Phi}) = \frac{1}{2} min\{eig(P), eig(\Gamma^{-1})\}(e^T e + \bar{\Phi}^T \bar{\Phi}), \tag{52}$$

then it can be derived that:

$$V \geq \alpha \geq 0, \quad \alpha(0) = 0, \tag{53}$$

which proves V is positive-definite.

Similarly, let:

$$\beta(e, \bar{\Phi}) = \frac{1}{2} max\{eig(P), eig(\Gamma^{-1})\}(e^T e + \bar{\Phi}^T \bar{\Phi}), \tag{54}$$

then it can be derived that:

$$V \leq \beta, \quad \beta(0) = 0, \tag{55}$$

which proves V is decrescent.

Also, as

$$||V|| \to \infty \quad as \quad ||(e^T, \bar{\Phi}^T)^T|| \to \infty, \tag{56}$$

V is radial unbounded, thus the system is uniformly stable in the large.

Also, $||e||$ and $||\dot{e}||$ are bounded, so e is globally asymptotically stable:

$$lim_{t\to\infty} e = 0. \tag{57}$$

3 Simulation using Simulink with square reference signal

In this section, tasks (b) and (c) are solved, where a Simulink model is built and simulations are performed accordingly.

The plant is simulated as:

$$\frac{Y(s)}{U(s)} = \frac{-0.5s - 1}{s^2 + 0.22s + 6.1}, \tag{58}$$

where $b_0 = -0.5$, $b_1 = -1$, $a_1 = 0.22$, and $a_2 = 6.1$. The damping ratio and natural frequency of the plant are calculated as 0.045 and 2.47.

The Simulink model is shown in Figure 1. Reference signal $r(t)$ is chosen as a square wave with amplitude $= 1$ and frequency $= 0.05$.

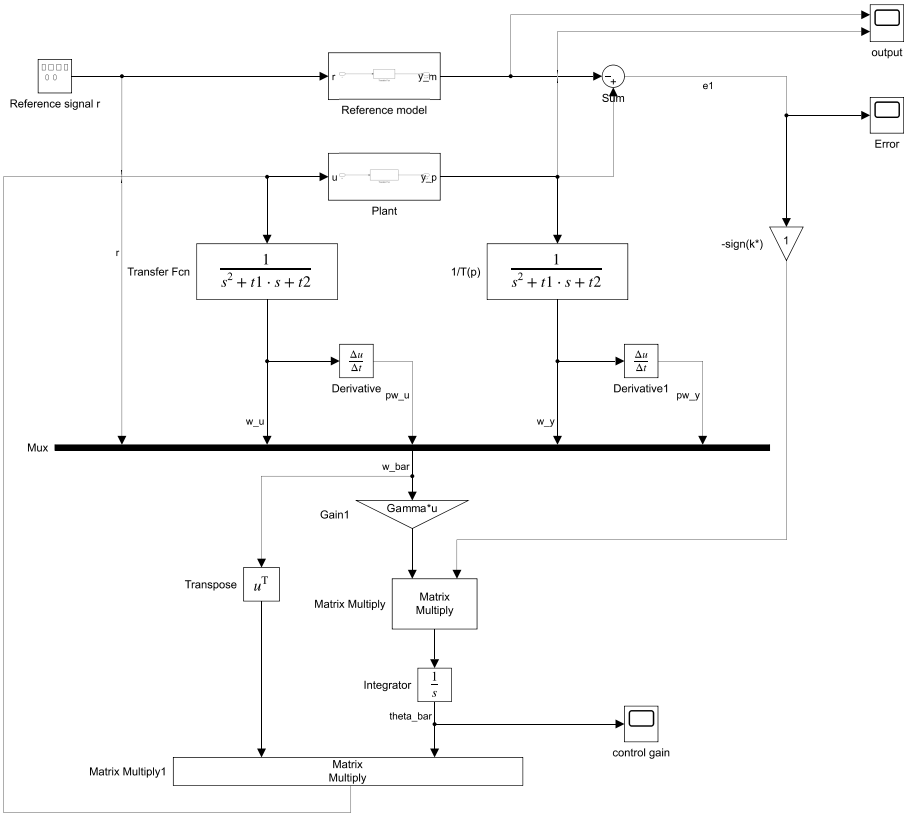

Figure 1: Simulink model of the model reference adaptive control system.

The MATLAB codes are attached as follows. Here the initial parameters are used, where τ is set to be 0.1, and for the filtering system $1/T(s)$, the damping ratio is set to be 0.045, and the natural frequency is set to be 2.47, which is the same as the plant model. As a result, $t_1 = 0.2223$ and $t_2 = 6.1$. The parameters will be changed later, to discover their effects on control results.

```
clc
clear all;

%%
mdl = "CA1_model";
open_system(mdl);

%%
% plant parameters (1) as given in the description
b0=-0.5;
b1=-1;
a1=0.22;
a2=6.1;
Kp=b0;
Zp=[1 b1/b0];
Rp=[1 a1 a2];

% reference model, parameters are self-defined
tau=1/10;
Rm=[1 1/tau];
Km=1/tau;

% filtering system 1/T(p)
C=0.045;
w=2.47;
T=[1 2*C*w w^2];
t1=T(2);
t2=T(3);

g=50;
Gamma=diag([10000*g,10000*g,1000*g,1000*g,1000*g]);

% theoretical result
[E, F]=deconv(conv(T, Rm), Rp);
Fbar=F/Kp;
Gbar=conv(E, Zp);
G1=Gbar-T;

K=Km/Kp;
% sequence in the model: [r, wu, pwu, wy, pwy]
theta_bar=[K,-G1(3),-G1(2),-Fbar(3),-Fbar(4)]
```

Using the initial parameters, the simulation results are shown in Figure 2, and the comparisons between adaptive control gains and "optimal" control gains are shown in Figure 3.

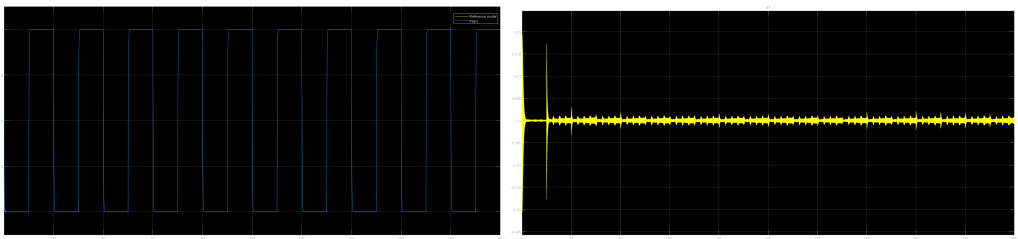

(a) Model outputs y and y_m (b) Tracking error e_1

Figure 2: Simulation results when $t_1 = 0.2223$ and $t_2 = 6.1$. (a) shows the plant output y and reference model output y_m, and (b) shows the tracking error e_1.

According to Figure 2, the output of the plant model tracks the output of the reference model well, with tracking error bounded and converges within 0.005.

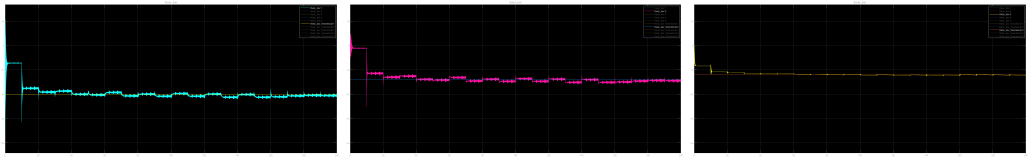

(a) k^* in $\bar{\theta}^*$ and in $\bar{\theta}(t)$. (b) $-g_2$ in $\bar{\theta}^*$ and in $\bar{\theta}(t)$. (c) $-g_1$ in $\bar{\theta}^*$ and in $\bar{\theta}(t)$.

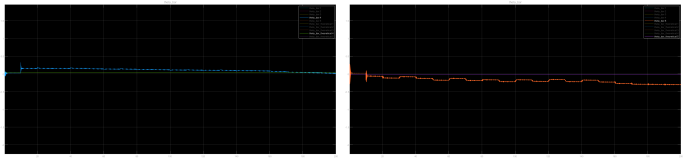

(d) $-f_2$ in $\bar{\theta}^*$ and in $\bar{\theta}(t)$. (e) $-f_1$ in $\bar{\theta}^*$ and in $\bar{\theta}(t)$.

Figure 3: Comparisons between theoretical optimal control gains and adaptive gains.

According to Figure 3, the adaptive gains are generally very close to the theoretical "optimal" control gains calculated using the plant model. In detail, for k^*, $-g_2$ and $-g_1$, the adaptive gains are initially 0, then quickly adapt to the optimal gains. For $-f_2$ and $-f_1$, as the theoretical optimal gains are very close to 0, the adaptive gains are initially very close to the optimal gains, then have some discrepancies. $-f_2$ then adapts back to the optimal gains, but $-f_1$ is keeping away from the optimal gains within the simulation period.

In the next subsection, different options of filtering parameters are explored.

3.1 Effects of the observer polynomial $T(p)$

In the previous simulation, $T(p)$ was chosen to have the same damping ratio and natural frequency as the plant model. As $t_1 = 0.2223$ and $t_2 = 6.1$, the poles of the filtering system can be calculated as $s = -0.11115 \pm 2.467i$. In this section, the value of damping ratio C and natural frequency w will be changed, thus t_1 and t_2 will be changed, in order to explore the effects of $T(p)$ on adaptive control performance.

3.1.1 Simulation when $C = 0.01$, $w = 2.47$

When $C = 0.01$, $w = 2.47$, $t_1 = 0.0494$, and $t_2 = 6.1$, the poles of this filtering system are $s = -0.0247 \pm 2.47i$, which is a stable system with slower decay to perturbations and with a slight increase in the oscillation frequency.

The simulation results are shown in Figure 4, and the comparisons between adaptive control gains and "optimal" control gains are shown in Figure 5.

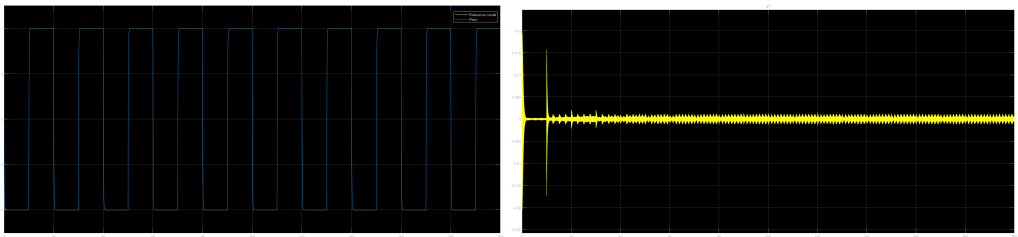

(a) Model outputs y and y_m (b) Tracking error e_1

Figure 4: Simulation results when $t_1 = 0.0494$ and $t_2 = 6.1$. (a) shows the plant output y and reference model output y_m, and (b) shows the tracking error e_1.

According to Figure 4, the output of the plant model tracks the output of the reference model well, with tracking error bounded and converges within 0.005. Compared with Figure 2b, the oscillation

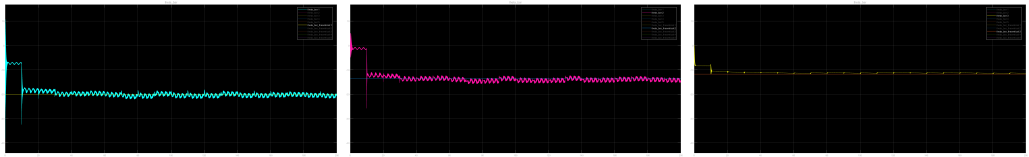

(a) k^* in $\bar{\theta}^*$ and in $\bar{\theta}(t)$. (b) $-g_2$ in $\bar{\theta}^*$ and in $\bar{\theta}(t)$. (c) $-g_1$ in $\bar{\theta}^*$ and in $\bar{\theta}(t)$.

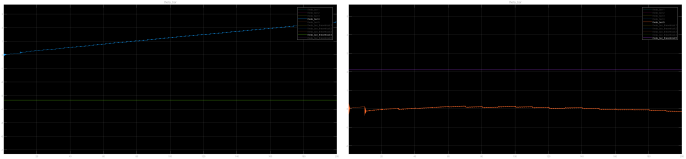

(d) $-f_2$ in $\bar{\theta}^*$ and in $\bar{\theta}(t)$. (e) $-f_1$ in $\bar{\theta}^*$ and in $\bar{\theta}(t)$.

Figure 5: Comparisons between theoretical optimal control gains and adaptive gains, when $t_1 = 0.0494$ and $t_2 = 6.1$.

frequency of the error signal in Figure 4b becomes slightly larger, which is consistent with the change on the filtering system.

According to Figure 5, the adaptive gains have different behaviors compared with Figure 3. In detail, for k^*, $-g_2$ and $-g_1$, the adaptive gains are initially 0, then quickly adapt to the optimal gains. For $-f_2$ and $-f_1$, the adaptive gains have some small discrepancies. $-f_2$ is initially close to the optimal gain, then away from the optimal gain. $-f_1$ is initially close to 0 and doesn't adapt to the optimal gain.

3.1.2 Simulation when $C = 0.1$, $w = 2.47$

When $C = 0.1$, $w = 2.47$, $t_1 = 0.494$, and $t_2 = 6.1$, the poles of this filtering system are $s = -0.247 \pm 2.457i$, which is a stable system with faster decay to perturbations and with a slight decrease in the oscillation frequency.

The simulation results are shown in Figure 6, and the comparisons between adaptive control gains and "optimal" control gains are shown in Figure 7.

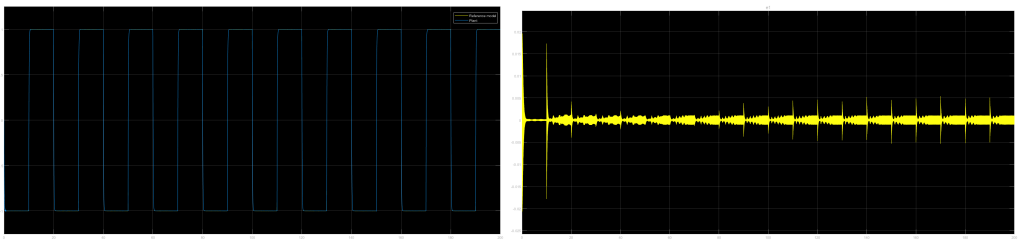

(a) Model outputs y and y_m (b) Tracking error e_1

Figure 6: Simulation results when $t_1 = 0.494$ and $t_2 = 6.1$. (a) shows the plant output y and reference model output y_m, and (b) shows the tracking error e_1.

According to Figure 6, the output of the plant model tracks the output of the reference model well, with tracking error bounded and converges within 0.005. Compared with Figure 2b and Figure 4b, the oscillation frequency of the error signal in Figure 6b becomes slightly slower, which is consistent with the change on the filtering system. However, the error signal in Figure 6b has some sparks when $t > 80s$, and tends to become severe.

According to Figure 7, the adaptive gains have different behaviors compared with previous simulations. In detail, for k^*, $-g_2$ and $-g_1$, the adaptive gains are initially 0. Although they quickly adapt to the optimal gains, there are some small discrepancies between the adapted gains and the optimal gains. For $-f_2$ and $-f_1$, $-f_2$ is initially close to the optimal gain, then away from the optimal gain. $-f_1$ is initially away from the optimal gain, then slowly adapts to the optimal gain.

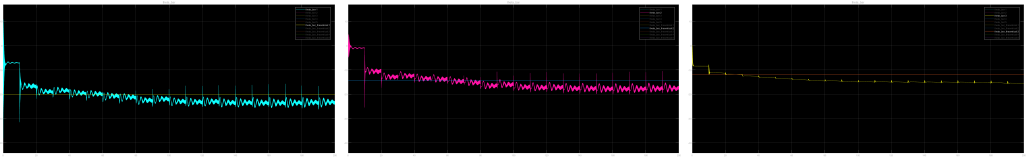

(a) k^* in $\bar{\theta}^*$ and in $\bar{\theta}(t)$. (b) $-g_2$ in $\bar{\theta}^*$ and in $\bar{\theta}(t)$. (c) $-g_1$ in $\bar{\theta}^*$ and in $\bar{\theta}(t)$.

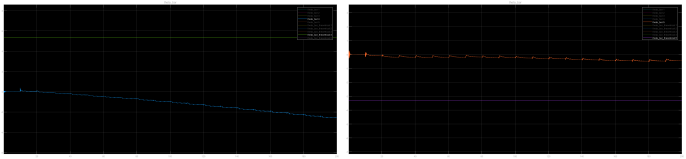

(d) $-f_2$ in $\bar{\theta}^*$ and in $\bar{\theta}(t)$. (e) $-f_1$ in $\bar{\theta}^*$ and in $\bar{\theta}(t)$.

Figure 7: Comparisons between theoretical optimal control gains and adaptive gains, when $t_1 = 0.494$ and $t_2 = 6.1$.

3.1.3 Simulation when $C = 0.045$, $w = 1.24$

When $C = 0.045$, $w = 1.24$, $t_1 = 0.1116$, and $t_2 = 1.5376$, the poles of this filtering system are $s = -0.0558 \pm 1.239i$, which is a stable system with a slight decrease in the oscillation frequency.

The simulation results are shown in Figure 8, and the comparisons between adaptive control gains and "optimal" control gains are shown in Figure 9.

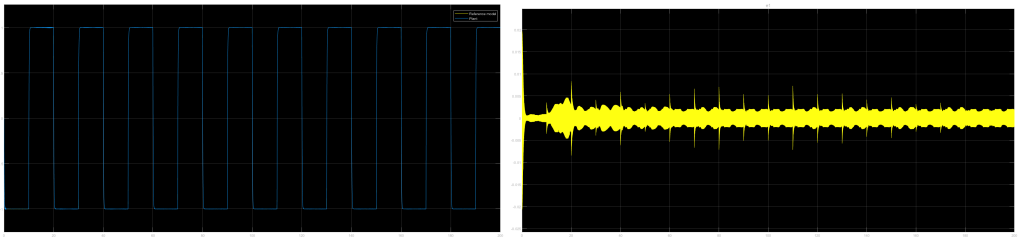

(a) Model outputs y and y_m (b) Tracking error e_1

Figure 8: Simulation results when $t_1 = 0.1116$ and $t_2 = 1.5376$. (a) shows the plant output y and reference model output y_m, and (b) shows the tracking error e_1.

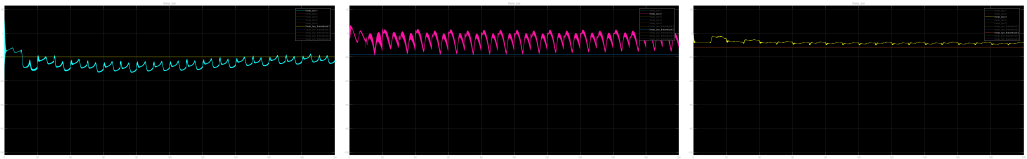

(a) k^* in $\bar{\theta}^*$ and in $\bar{\theta}(t)$. (b) $-g_2$ in $\bar{\theta}^*$ and in $\bar{\theta}(t)$. (c) $-g_1$ in $\bar{\theta}^*$ and in $\bar{\theta}(t)$.

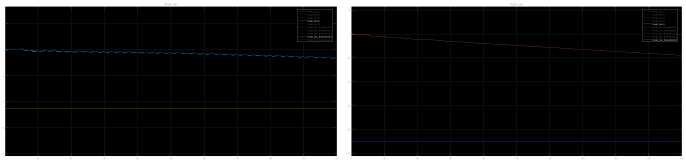

(d) $-f_2$ in $\bar{\theta}^*$ and in $\bar{\theta}(t)$. (e) $-f_1$ in $\bar{\theta}^*$ and in $\bar{\theta}(t)$.

Figure 9: Comparisons between theoretical optimal control gains and adaptive gains, when $t_1 = 0.1116$ and $t_2 = 1.5376$.

According to Figure 8, the output of the plant model tracks the output of the reference model well, with tracking error bounded and converges within 0.005. Compared with Figure 2b, 4b and 6b, the

oscillation frequency of the error signal in Figure 8b becomes even slower, which is consistent with the change on the filtering system. However, the error signal in Figure 8b has some sparks, and the absolute error value is larger than previous simulations.

According to Figure 9, the adaptive gains have different behaviors compared with previous simulations. In detail, for k^*, $-g_2$ and $-g_1$, the adaptive gains are initially 0. Although they quickly adapt to the optimal gains, there are some small discrepancies between the adapted gains and the optimal gains. For $-f_2$ and $-f_1$, both of them are initially away from the optimal gains, then slowly adapt to the optimal gains. However, until the simulation ends at $t = 200s$, the distances are still large.

3.1.4 Simulation when $C = 0.045$, $w = 4.94$

When $C = 0.045$, $w = 4.94$, $t_1 = 0.4446$, and $t_2 = 24.4$, the poles of this filtering system are $s = -0.2223 \pm 4.93i$, which is a stable system with an increase in the oscillation frequency.

The simulation results are shown in Figure 10, and the comparisons between adaptive control gains and "optimal" control gains are shown in Figure 11.

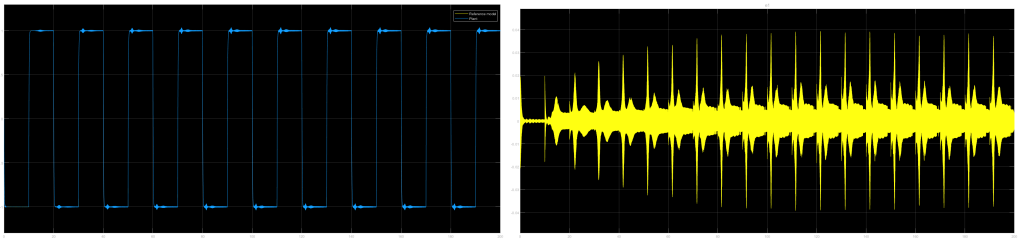

(a) Model outputs y and y_m (b) Tracking error e_1

Figure 10: Simulation results when $t_1 = 0.4446$ and $t_2 = 24.4$. (a) shows the plant output y and reference model output y_m, and (b) shows the tracking error e_1.

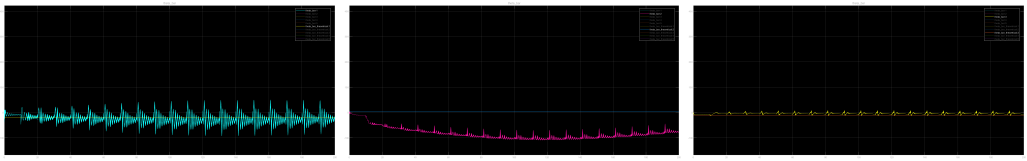

(a) k^* in $\bar{\theta}^*$ and in $\bar{\theta}(t)$. (b) $-g_2$ in $\bar{\theta}^*$ and in $\bar{\theta}(t)$. (c) $-g_1$ in $\bar{\theta}^*$ and in $\bar{\theta}(t)$.

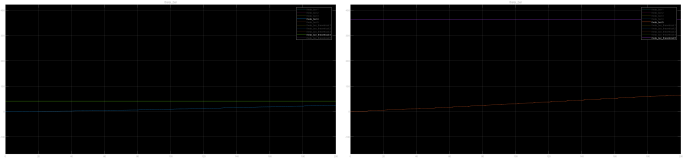

(d) $-f_2$ in $\bar{\theta}^*$ and in $\bar{\theta}(t)$. (e) $-f_1$ in $\bar{\theta}^*$ and in $\bar{\theta}(t)$.

Figure 11: Comparisons between theoretical optimal control gains and adaptive gains, when $t_1 = 0.4446$ and $t_2 = 24.4$.

According to Figure 10, the output of the plant model tracks the output of the reference model worse than previous simulations, with large tracking errors. Compared with Figure 2b, 4b, 6b, and 8b, the error signal in Figure 10b has faster oscillation frequency, and has some large sparks, and the absolute error value is significantly larger than previous simulations.

According to Figure 11, the adaptive gains have different behaviors compared with previous simulations. In detail, k^* and $-g_1$ adapt to the optimal gain, but with a large oscillation frequency. $-g_2$ first moves away then adapts to the optimal gain, also with a large oscillation frequency. $-f_2$ and $-f_1$ slowly adapt to the optimal gains. However, until the simulation ends at $t = 200s$, the distance between $-f_1$ and the optimal gain is still large.

3.1.5 Summary on the effect of observer polynomial

According to the simulations conducted using the initial parameters and the parameters in sections 3.1.1 - 3.1.4, a summary can be concluded here.

When C becomes smaller, t_1 becomes smaller, and the real-parts of the poles of the filtering system are closer to the origin, then the filtering system has slower decay to perturbations; the imaginary-parts of the poles are away from the origin, then the filtering system has a slight increase in the oscillation frequency.

When C becomes larger, t_1 becomes larger, and the real-parts of the poles of the filtering system are away from the origin, then the filtering system has faster decay to perturbations; the imaginary-parts of the poles are closer to the origin, then the filtering system has a slight decrease in the oscillation frequency. However, as t_1 becomes larger, more sparks appear in the error signal.

When w becomes smaller, both t_1 and t_2 become smaller, and both the real-parts and imaginary-parts of the poles of the filtering system are closer to the origin, then the filtering system has slower decay to perturbations and a decrease in the oscillation frequency.

When w becomes larger, both t_1 and t_2 become larger, and both the real-parts and imaginary-parts of the poles of the filtering system are away from the origin, then the filtering system has faster decay to perturbations and an increase in the oscillation frequency, and more sparks appear in the error signal.

In summary, comparing all simulation results, the best choice for $T(p)$ is $p^2 + 0.2223p + 6.1$, which is used for task (d) in the next section.

4 Simulation with sinusoidal reference signal

In this section, task (d) is solved, where the reference signals become sinusoidal.

First, the reference signal is a single sinusoid:

$$r = 10sin(0.5t), \tag{59}$$

the amplitude is 10 and frequency is $0.0796Hz$. Using $T(p) = p^2 + 0.2223p + 6.1$, the simulation results are shown in Figure 12, and the comparisons between adaptive control gains and "optimal" control gains are shown in Figure 13.

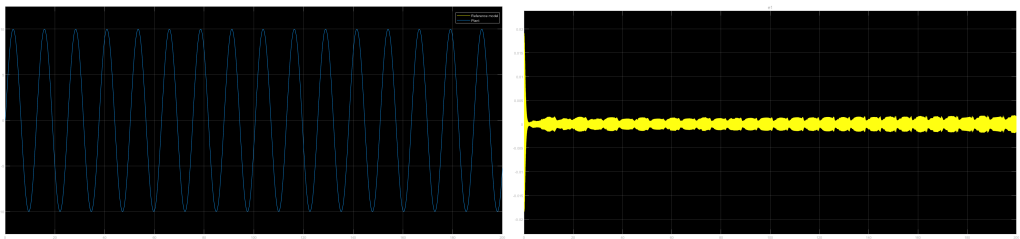

(a) Model outputs y and y_m (b) Tracking error e_1

Figure 12: Simulation results when $T(p) = p^2 + 0.2223p + 6.1$, and $r = 10sin(0.5t)$. (a) shows the plant output y and reference model output y_m, and (b) shows the tracking error e_1.

According to Figure 12, the output of the plant model tracks the output of the reference model well. The absolute value of error is slightly larger than the error in Figure 2b, but still bounded and converges within 0.005.

According to Figure 13, the gains adaptations are not so ideal compared with gains in Figure 3. Both k^*, $-g_2$, $-g_1$ and $-f_1$ have a trend to decrease. Although they adapt to the optimal gains at first, the decrease doesn't stop and they continue to move away from the optimal gains. Instead, $-f_2$ adapts to the optimal gain well.

More simulations are to be carried out in the following subsections, to get valid conclusions.

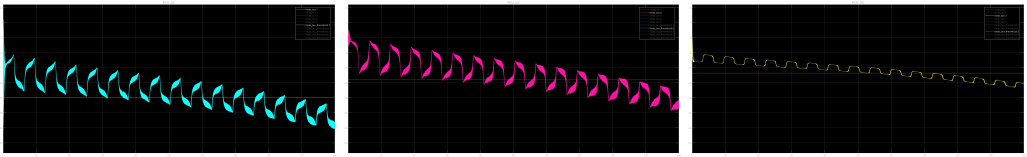

(a) k^* in $\bar{\theta}^*$ and in $\bar{\theta}(t)$. (b) $-g_2$ in $\bar{\theta}^*$ and in $\bar{\theta}(t)$. (c) $-g_1$ in $\bar{\theta}^*$ and in $\bar{\theta}(t)$.

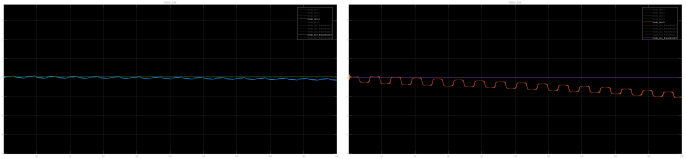

(d) $-f_2$ in $\bar{\theta}^*$ and in $\bar{\theta}(t)$. (e) $-f_1$ in $\bar{\theta}^*$ and in $\bar{\theta}(t)$.

Figure 13: Comparisons between theoretical optimal control gains and adaptive gains, when $T(p) = p^2 + 0.2223p + 6.1$, and $r = 10sin(0.5t)$.

4.1 Comparison with square reference signals

In this section, a square reference signal with similar amplitude and frequency is used for simulation. The amplitude is chosen to be 10, and the frequency is chosen to be $0.0796Hz$. The simulation results when $T(p) = p^2 + 0.2223p + 6.1$ are shown in Figure 14.

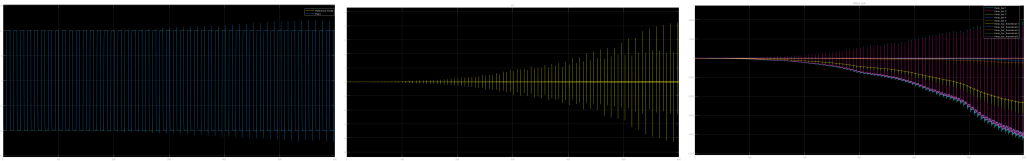

(a) Model outputs y and y_m (b) Tracking error e_1 (c) Control gains $\bar{\theta}$

Figure 14: Simulation results when $T(p) = p^2 + 0.2223p + 6.1$, and reference signal is a square wave with amplitude $= 10$ and frequency $= 0.0796Hz$. (a) shows the plant output y and reference model output y_m, (b) shows the tracking error e_1, and (c) shows the control gains $\bar{\theta}$.

It can be observed that, as time progresses, the spark of the error signal becomes larger and larger, and the adaptive control gains become further and further away from the optimal gains. Compared with the results in Figure 12, the square wave case is much worse.

According to the conclusions made in Section 3, when the error signal has severe sparks, we can set smaller t_1 and t_2 to reduce the sparks. A new simulation using $T(p) = p^2 + 0.022p + 1.21$ is conducted, and the results are shown in Figure 15.

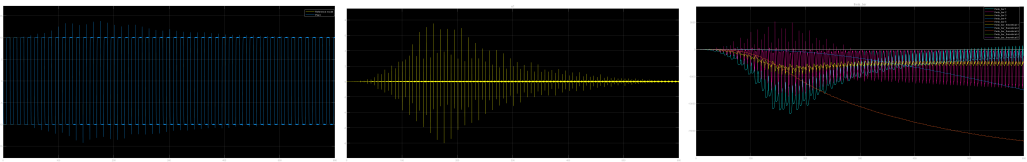

(a) Model outputs y and y_m (b) Tracking error e_1 (c) Control gains $\bar{\theta}$

Figure 15: Simulation results when $T(p) = p^2 + 0.022p + 1.21$, and reference signal is a square wave with amplitude $= 10$ and frequency $= 0.0796Hz$. (a) shows the plant output y and reference model output y_m, (b) shows the tracking error e_1, and (c) shows the control gains $\bar{\theta}$.

It can be observed that, as time progresses, although the spark of the error signal becomes larger at first, it reduces later and the error signal converges. The adaptive control gains become further away from the optimal gains at first, but most of them then adapt back to the optimal gains later.

4.2 Comparison with additive sinusoidal reference signals

In this section, the reference signal is a sum of multiple sinusoidal signals with different but comparable periods and amplitude. The sub-signals are chosen to be:

$$r_1 = r = 10sin(0.5t); \tag{60}$$

$$r_2 = 9sin(0.6t); \tag{61}$$

$$r_3 = 12sin(0.4t); \tag{62}$$

$$r_4 = 8cos(0.55t); \tag{63}$$

$$r_5 = 11cos(0.45t). \tag{64}$$

The simulation results are shown in Figure 16. It can be observed that the output of the plant model tracks the output of the reference model well, but the absolute value of the error signal is larger than the error signal in Figure 12b.

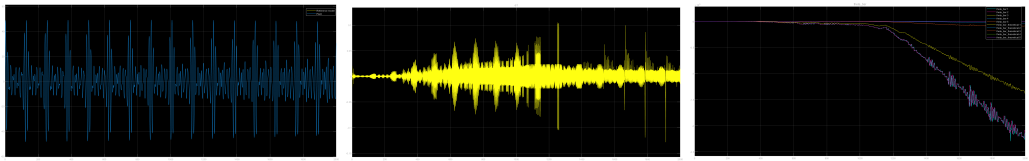

(a) Model outputs y and y_m (b) Tracking error e_1 (c) Control gains $\bar{\theta}$

Figure 16: Simulation results when $T(p) = p^2 + 0.2223p + 6.1$, and reference signal is the sum of 5 sinusoidal signals. (a) shows the plant output y and reference model output y_m, (b) shows the tracking error e_1, and (c) shows the control gains $\bar{\theta}$.

The relationship between the summed signal and the sub-signals is also explored. r_1 to r_5 are used as reference signals separately, then the outputs, errors and control gains are added together for all five signals, to be compared with the results in Figure 16. The intermediate steps are omitted, and the results are shown in Figure 17.

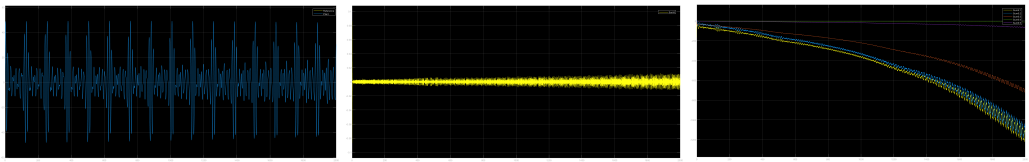

(a) Model outputs y and y_m (b) Tracking error e_1 (c) Control gains $\bar{\theta}$

Figure 17: Simulation results that the output, error and control gains are the sum of 5 sub-systems. (a) shows the plant output y and reference model output y_m, (b) shows the tracking error e_1, and (c) shows the control gains $\bar{\theta}$.

Comparing Figure 16a and Figure 17a, the outputs of both conditions are exactly the same. However, comparing Figure 16b and Figure 17b, the error signals are very different. Comparing Figure 16c and Figure 17c, the control gains are also very different, so the system doesn't satisfy superposition.

The reason why the system doesn't satisfy superposition maybe because the system is a non-linear system. In a non-linear adaptive system, the system may adjust its parameters or structure based on the characteristics of the input signal, and this dynamic change may cause the overall response of the system to be inconsistent with the expected linear superposition. Moreover, the summed signal is much more complex than its 5 components, then the difficulty to control the system using the summed signal is higher than to control the sub-systems separately and add them up. This explains why the error signal in Figure 16b is larger than the error signal in Figure 17b.

5 Simulation with changed plant

In this section, task (e) is solved, where the plant is initially

$$\frac{Y(s)}{U(s)} = \frac{-0.5s - 1}{s^2 + 0.22s + 6.1}, \tag{65}$$

and changes to

$$\frac{Y(s)}{U(s)} = \frac{-2s - 5}{s^2 + 20.4s + 6.4}, \tag{66}$$

when $t \geq 100$.

The Simulink model is shown in Figure 18. Reference signal $r(t)$ is chosen as a square wave with amplitude $= 1$ and frequency $= 0.05$.

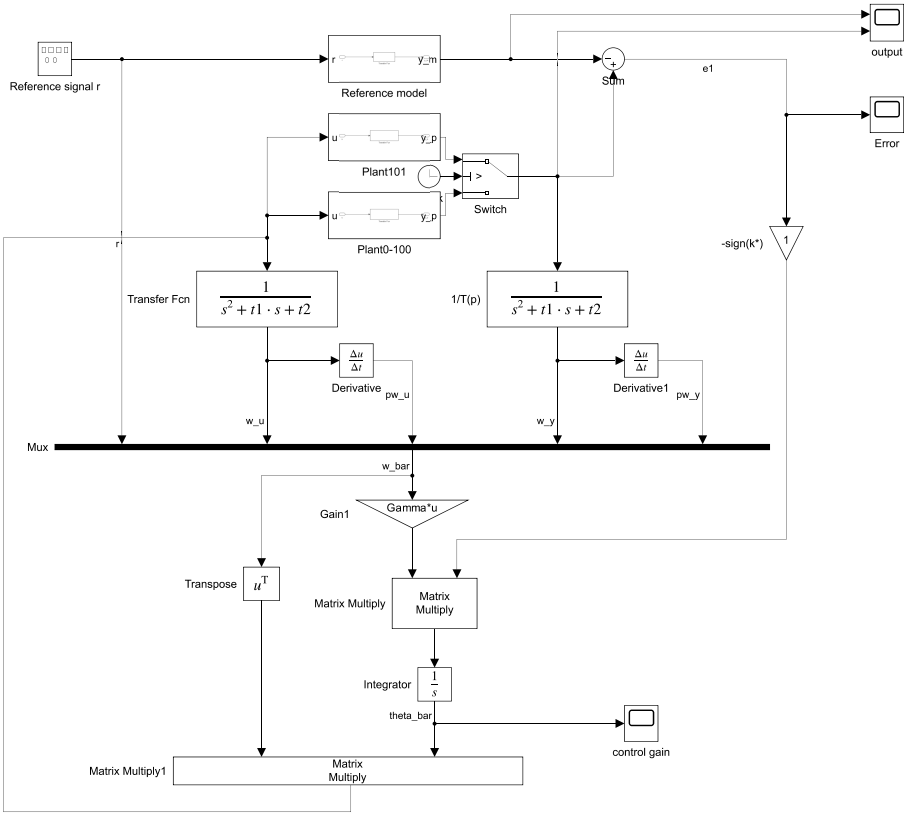

Figure 18: Simulink model of the change plant simulation.

The MATLAB codes are attached as follows.

```
clc
clear all;

%%
mdl = "CA1_model_change";
open_system(mdl);

%%
% plant parameters (1) as given in the description
b0=-0.5;
b1=-1;
a1=0.22;
```

```
a2=6.1;
Kp=b0;
Zp=[1 b1/b0];
Rp=[1 a1 a2];

% changed plant
b00=-2;
b11=-5;
a11=20.4;
a22=6.4;

% reference model, parameters are self-defined
tau=1/10;
Rm=[1 1/tau];
Km=1/tau;

C=0.045;
w=2.47;
T=[1 2*C*w w^2];
t1=T(2);
t2=T(3);

num=[b0 b1];
dem=[1 2*C*w w^2];
sys=tf(num, dem);
pole(sys)

g=50;
Gamma=diag([10000*g,10000*g,1000*g,1000*g,1000*g]);

% theoretical
[E, F]=deconv(conv(T, Rm), Rp);
Fbar=F/Kp;
Gbar=conv(E, Zp);
G1=Gbar-T;

K=Km/Kp;
theta_bar=[K,-G1(3),-G1(2),-Fbar(3),-Fbar(4)]
```

The simulation results are shown in Figure 19.

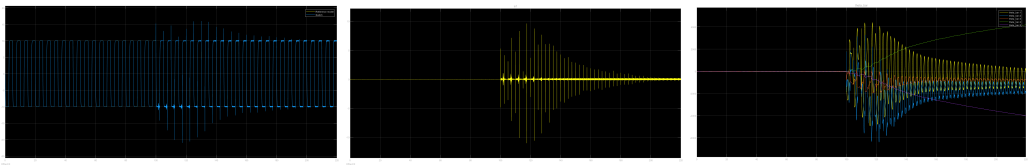

(a) Model outputs y and y_m (b) Tracking error e_1 (c) Control gains $\bar{\theta}$

Figure 19: Simulation results for plant change problem. (a) shows the plant output y and reference model output y_m, (b) shows the tracking error e_1, and (c) shows the control gains $\bar{\theta}$.

According to Figure 19a and 19b, the output of the plant model tracks the output of the reference model well when $t < 100$. When $t \geq 100$, the plant parameters change, a sharp perturbation appears and there are significant sparks in the error signal. When $t > 200$, the sparks almost disappear, and the error signal converges, with slightly larger absolute value. It proves that the designed adaptive controller is working well on such a sudden plant change.

References

[1] Briefing Notes for CA1: Adaptive Control of a Second Order Plant with Output Feedback.

[2] Lecture Notes of EE5104/6104 Advanced/Adaptive Control Systems.